

# Microburst Scale Size Derived from Multiple Bounces of a Microburst Simultaneously Observed with the FIREBIRD-II CubeSats

Mykhaylo Shumko<sup>1</sup>, John Sample<sup>1</sup>, Arlo Johnson<sup>1</sup>, Bern Blake<sup>2</sup>, Alex Crew<sup>3</sup>, Harlan Spence<sup>4</sup>, David Klumpar<sup>1</sup>, Oleksiy Agapitov<sup>5</sup>, Matthew Handley<sup>1</sup>

<sup>1</sup>Department of Physics, Montana State University, Bozeman, Montana, USA

<sup>2</sup>Space Science Applications Laboratory, The Aerospace Corporation, Los Angeles, California, USA

<sup>3</sup>The Johns Hopkins University Applied Physics Laboratory LLC, Laurel, Maryland, USA

<sup>4</sup>Institute for the Study of Earth, Oceans, and Space, University of New Hampshire, Durham, New Hampshire, USA

<sup>5</sup>Space Sciences Laboratory, UC Berkeley, Berkeley, California, USA

## Key Points:

- Multiple bounces from a microburst were observed by the two FIREBIRD-II CubeSats at LEO.
- The lower bounds on the microburst scale size at LEO were  $29 \pm 1$  km (latitudinal) and  $51 \pm 11$  km (longitudinal).
- Deduced lower bound equatorial scale size was similar to the whistler-mode chorus source scale.

## Abstract

We present the observation of a spatially large microburst with multiple bounces made simultaneously by the FIREBIRD-II CubeSats on February 2nd, 2015. This is the first observation of a microburst with a subsequent decay made by two co-orbiting but spatially separated spacecraft. From these unique measurements, we place estimates on the lower bounds of the spatial scales as well as quantify the electron bounce periods. The microburst's lower bound latitudinal scale size was  $29 \pm 1$  km and the longitudinal scale size was  $51 \pm 1$  km in low earth orbit. We mapped these scale sizes to the magnetic equator and found that the radial and azimuthal scale sizes were at least  $500 \pm 10$  km and  $530 \pm 10$  km, respectively. These lower bound equatorial scale sizes are similar to whistler-mode chorus wave source scale sizes, which supports the hypothesis that microbursts are a product of electron scattering by chorus waves. Lastly, we estimated the bounce periods for 200-800 keV electrons and found good agreement with four common magnetic field models.

## 1 Introduction

The dynamics of radiation belt electrons are complex, and are driven by competition between source and loss processes. A few possible loss processes are radial diffusion [Shprits and Thorne, 2004], magnetopause shadowing [Ukhorskiy *et al.*, 2006], and pitch angle and energy diffusion due to scattering of electrons by plasma waves [e.g. Abel and Thorne, 1998; Summers *et al.*, 1998; Meredith *et al.*, 2002; Selesnick *et al.*, 2003; Horne and Thorne, 2003; Thorne *et al.*, 2005; Mozer *et al.*, 2018]. There are a variety of waves that cause pitch angle scattering, including electromagnetic ion cyclotron waves, plasmaspheric hiss, and chorus [Millan and Thorne, 2007; Thorne, 2010]. Chorus predominantly occurs in the dawn sector (6-12 magnetic local times (MLT)) [Li *et al.*, 2009] where it accelerates electrons with large equatorial pitch angles and scatters electrons with small equatorial pitch angles [Horne and Thorne, 2003]. Some of these electrons may be impulsively scattered into the loss cone, where they result in short-duration ( $\sim 100$  ms) enhancements in precipitating flux called microbursts.

Anderson and Milton [1964] coined the term microburst to describe high altitude balloon observations of  $\sim 100$  ms duration enhancements of bremsstrahlung X-rays emitted from scattered microburst electrons impacting the atmosphere. Since then, non-relativistic (less than a few hundred keV) microbursts have been routinely observed with other balloon missions [e.g. Parks, 1967; Woodger *et al.*, 2015; Anderson *et al.*, 2017]. A review of the

literature shows no reports of microbursts above a few hundred keV observed by balloons [Millan *et al.*, 2002; Woodger *et al.*, 2015]. This lack of observation may be explained by relatively weaker pitch angle scattering of relativistic electrons by chorus [Lee *et al.*, 2012].

In addition to the X-ray signature ~~(Deleted: proxy)~~ for bursts of electron precipitation, the precipitating relativistic and non-relativistic electrons have been measured in situ by spacecraft orbiting in low earth orbit (LEO). Hereinafter, we refer to these electron signatures observed by LEO spacecraft also as microbursts. Microbursts have been observed with, e.g. the Solar Anomalous and Magnetospheric Particle Explorer's (SAMPEX) > 150 keV and > 1 MeV channels [Nakamura *et al.*, 1995, 2000; Blake *et al.*, 1996; Lorentzen *et al.*, 2001a,b; O'Brien *et al.*, 2003, 2004; Blum *et al.*, 2015] and Focused Investigation of Relativistic Electron Bursts: Intensity, Range, and Dynamics (FIREBIRD-II) with its > 200 keV energy channels [Crew *et al.*, 2016; Anderson *et al.*, 2017; Breneman *et al.*, 2017]. ~~(Deleted: To characterize the source of microbursts, Lorentzen *et al.*, 2001 found that microbursts and chorus waves predominantly occur in the dawn sector and Breneman *et al.*, 2017 made a direct observational link between individual microbursts and chorus elements.)~~

~~(Added: Understanding microburst precipitation and its scattering mechanism is important to radiation belt dynamics. The scattering mechanism has been observationally studied by e.g. Lorentzen *et al.* [2001b] who found that microbursts and chorus waves predominantly occur in the dawn sector and Breneman *et al.* [2017] made a direct observational link between individual microbursts and chorus elements. Microbursts have been modeled and empirically estimated to be capable of depleting the relativistic electron population in the outer radiation belt on the order of a day [O'Brien *et al.*, 2004; Thorne *et al.*, 2005; Shprits *et al.*, 2007; Breneman *et al.*, 2017].)~~ An important parameter in this estimation of instantaneous radiation belt electron losses due to microbursts is their scale size. Parks [1967] used balloon measurements of bremsstrahlung X-rays to estimate the high altitude scale size of predominantly low energy microbursts to be  $40 \pm 14$  km. In Blake *et al.* [1996] a microburst with multiple bounces was observed by SAMPEX, and the microburst's latitudinal scale size in LEO was estimated to have been "at least a few tens of kilometers". Blake *et al.* [1996] concluded that typically microbursts are less than a few tens of electron gyroradii in size (at  $L = 5$  at LEO, the gyroradii of 1 MeV electrons is on the order of 100 m). Dietrich *et al.* [2010] used SAMPEX along with ground-based very low frequency stations to conclude that during one SAMPEX pass, the observed microbursts had scale sizes less than 4 km.

Since February 1st, 2015, microbursts have been observed by FIREBIRD-II, a pair of CubeSats in LEO. Soon after launch, when the two FIREBIRD-II spacecraft were at close range, a microburst with a scale size greater than 11 km was observed [Crew *et al.*, 2016]. On the same day, FIREBIRD-II simultaneously observed a microburst with multiple bounces. The microburst decay was observed over a period of a few seconds, while the spacecraft were traveling predominantly in latitude. Here we present the analysis and results of the latitude and longitude scale sizes and bounce periods of the first microburst with multiple bounces observed with the two FIREBIRD-II spacecraft.

## 2 Spacecraft and Observation

The FIREBIRD missions are comprised of a pair of identically-instrumented 1.5U CubeSats (15 x 10 x 10 cm) that are designed to measure electron precipitation in LEO [Spence *et al.*, 2012; Klumpar *et al.*, 2015]. The second mission, termed FIREBIRD-II, was launched on January 31st 2015. The two FIREBIRD-II CubeSats, identified as Flight Unit 3 (FU3) and Flight Unit 4 (FU4), were placed (Added: in a) 632 km apogee, 433 km perigee, and 99° inclination orbit [Crew *et al.*, 2016]. FU3 and FU4 are orbiting in a string of pearls configuration with FU4 ahead, to resolve the space-time ambiguity of (Replaced: events that are either spatial or temporal) replaced with: microbursts). Each FIREBIRD-II unit has two solid state detectors: one is mounted essentially at the spacecraft surface, covered only by a thin foil acting as a sun shade, with a field of view of 90° (surface detector), and the other is beneath a collimator which restricts the field of view to 54° (collimated detector). Only FU3 has a functioning surface detector, so this analysis utilizes the collimated detectors. FU3's surface and collimated detectors, as well as FU4's collimated detector observe electron fluxes in six energy channels from ~ 230 keV to > 1 MeV. (Added: FIREBIRD-II's High Resolution (HiRes) electron flux data is gathered) with an adjustable sampling (Replaced: rate replaced with: period) of 18.75 ms by default and (Added: can be) as fast as 12.5 ms.

On February 2nd, 2015 at 06:12 UT, both FIREBIRD-II spacecraft simultaneously observed an initial microburst, followed by subsequent periodic electron enhancements of diminishing amplitude shown in Fig. 1. This is thought to be the signature of a single burst of electrons, some of which precipitate, but the rest mirror near the spacecraft then bounce to the conjugate hemisphere where they mirror again (Added: and the subsequent bounces) produce a train of decaying peaks [Blake *et al.*, 1996; Thorne *et al.*, 2005]. This bounce signature occurred during the transition between the main and recovery phases of a storm

with a minimum Dst of -44 nT ( $K_p = 4$ , and  $AE \approx 400$  nT). At this time, the ~~(Replaced: High Resolution (HiRes)-electron flux~~ replaced with: **HiRes data**) was sampled at 18.75 ms. Five peaks were observed by both spacecraft. The fifth peak observed by FU4 was comparable to the Poisson noise and was not used in this analysis. This microburst was observed from the first energy channel ( $\approx 200 - 300$  keV), to the fourth energy channel ( $\approx 500 - 700$  keV), and FU3's surface detector observed the microburst up to the fifth energy channel (683 - 950 keV).

The HiRes data in Fig. 1 shows signs of energy dispersion, characterized by higher energy electrons arriving earlier than the lower energies. This time of flight energy dispersion tends to smear out the initial sharp burst upon each subsequent bounce. The first peak does not appear to be dispersed, and subsequent peaks show a dispersion trend consistent across energy channels. The black vertical bars have been added to Fig. 1 to highlight this energy dispersion. This dispersion signature and amplitude decay implies that the first peak was observed soon after the electrons were scattered, followed by decaying bounces.

At this time, in magnetic coordinates, FIREBIRD-II was at McIlwain  $L = 4.7$  and  $MLT = 8.3$ , calculated with the Tsyganenko 1989 (T89) magnetic field model [Tsyganenko, 1989] using IRBEM-Lib [Boscher *et al.*, 2012]. Geographically, they were above Sweden, latitude =  $63^\circ\text{N}$ , longitude =  $15^\circ\text{E}$ , altitude = 650 km. This geographic location is magnetically conjugate to the east of the so-called South Atlantic Anomaly (SAA). The SAA is the location where the mirror points of electrons tend to occur at locations deeper in the atmosphere owing to the offset of the dipole magnetic field from the Earth's center. ~~(Replaced: Electrons that encounter the SAA are removed from their eastward longitudinal drift paths [Comess *et al.*, 2003; Dietrich *et al.*, 2010]. This loss effect is termed the drift loss cone (DLC);~~ replaced with: **Electrons with pitch angles within the drift loss cone (DLC) will encounter the SAA and be removed from their eastward longitudinal drift paths [Comess *et al.*, 2013; Dietrich *et al.*, 2010].** FU3 and FU4 are therefore both in regions where the particles in the DLC have recently precipitated, leaving only particles that were recently scattered. At the spacecraft location, locally mirroring electrons would have mirrored at 95 km in the opposite hemisphere, with more field aligned electrons mirroring at even lower altitudes. From the analysis done by Fang *et al.* [2010], the peak in the total ionization rate in the atmosphere for 100 keV electrons is around 80 km altitude, while the total ionization rate from 1 MeV electrons peaks around 60 km altitude. It is, therefore, expected that a fraction of the microburst electrons will survive each encounter with the atmosphere. By plotting the peak flux

as a function of bounce (not shown), it was found that 40 - 60 % of the microburst electrons were lost on the first bounce, similar to the 33% loss per bounce observed for a bouncing microburst observed by SAMPEX [Thorne *et al.*, 2005].

### 3 Analysis

At the beginning of the FIREBIRD-II mission, two issues prevented the proper analysis of the microburst's spatial scale size: the spacecraft clocks were not synchronized, and their relative positions were not accurately known. We addressed these issues with a cross-correlation time lag analysis described in detail in the supporting information (SI). From this analysis, the time correction was  $2.28 \pm 0.12$  s (applied to Fig. 1) and the separation was  $19.9 \pm 0.9$  km at the time of the microburst observation.

#### 3.1 Electron Bounce Period

We used this unique observation of bouncing electrons to calculate the bounce period,  $t_b$  as a function of energy and compare it to (Added: the energy-dependent)  $t_b$  (Added: curves) derived from four magnetic field models, (Added: the results of which are shown in Fig. 2). The observed  $t_b$  and uncertainties were calculated by fitting the baseline-subtracted HiRes flux. The baseline flux used in this analysis is given in O'Brien *et al.* [2004] as the flux at the 10th percentile over a specified time interval, which in this analysis was taken to be 0.5 seconds. The flux was fitted with a superposition of Gaussians for each energy channel, and the uncertainty in flux was calculated using the Poisson error from the microburst and baseline fluxes summed in quadrature. Using the fit parameters, the mean  $t_b$  for the lowest four energy channels is shown in Fig. 2. The trend of decreasing  $t_b$  as a function of energy is evident in Fig. 2, which further supports the assumption that the subsequent peaks are bounces, and not a train of microbursts scattered by bouncing chorus.

The decaying peaks in the 231-408 keV electron flux observed by FU3's lowest two energy channels (see Fig. 1) were right-skewed. One explanation is that there was in-channel energy dispersion within those channels. (Deleted: that is smeared out by the broad energy channels-) Since  $t_b$  of higher energy electrons is shorter, a right-skewed peak implies that higher energy electrons were more abundant within that channel (Added: e.g. in FU3's 231-300 keV channel, the 300 keV electrons will arrive sooner than the 231 keV electrons, but will they will be binned in the same channel). A Gaussian fit cannot account for this in-

channel dispersion, and as a first order correction, minima between peaks was used to calculate  $t_b$ , and is shown in Fig. 2. The observed energy-dependent dispersion shown in Fig. 2 is consistent with higher energy peaks returning sooner. This dispersion consistency further supports the assumption that the subsequent peaks are bounces, and not a train of microbursts scattered by bouncing chorus.

To compare the observed and modeled  $t_b$ , we superposed  $t_b$  curves for various models including an analytical solution in a dipole [Schulz and Lanzerotti, 1974], and numerical models: T89, Tsyganenko 2004 (T04) [Tsyganenko and Sitnov, 2005], and Olson & Pfizter Quiet [Olson and Pfizter, 1982] in Fig. 2. The numerical  $t_b$  curves were calculated using a wrapper for IRBEM-Lib. This code traces the magnetic field line between mirror points, and calculates  $t_b$  assuming conservation of energy and the first adiabatic invariant for electrons mirroring at FIREBIRD-II. With the empirical  $t_b$ , the models agree within FIREBIRD-II's uncertainties, but the T04 model has the largest discrepancy compared to the other models.

### 3.2 Microburst Energy Spectra

Next, we investigated the energy spectra of this microburst. The energy spectra was modeled with an exponential that was fit to the peak flux derived from the Gaussian fit parameters in section 3.1 to all but the highest energy channel. We found that the E-folding energy,  $E_0 \sim 100$  keV. ~~(Replaced: This spectra is similar to the spectra shown in Lee et al., [2005] who used STSAT-1 and Datta et al. [1997] who used a sounding rocket.~~ replaced with: This spectra is similar to spectra show by Lee et al. [2005] from STSAT-1 and Datta et al. [1997] from sounding rocket measurements.) The energy spectra is soft for a typical microburst observed with FIREBIRD-II and there was no statistically significant change in  $E_0$  for subsequent bounces.

### 3.3 Microburst Scale Sizes

Lastly, after we applied the ~~(Added: time and separation)~~ corrections detailed in the SI, we mapped the locations of FU3 and FU4 in Fig. 3. The locations where FU3 saw peaks 1-5 and where FU4 saw peaks 1-4 are shown as P1-5 and P1-4, respectively. The lower bound on the latitudinal extent of the microburst was the difference in latitude between P1 on FU3 and P4 on FU4 and was found to be  $29 \pm 1$  km. The uncertainty was estimated from the

spacecraft separation uncertainty described in the SI. This scale size is the largest reported by FIREBIRD-II.

(Added: In section 3.1, we showed that the observed decaying peaks were likely due to bouncing, so we assume that the observed electrons in subsequent bounces were the drifted electrons from the initial microburst.) (Replaced: ~~To calculate the longitudinal scale size of the microburst, we assumed that~~ replaced with: Under this assumption,) the scattered electrons observed in the last bounce by FIREBIRD-II, must have drifted east from their initial scattering longitude, (Added: allowing us to calculate the minimum longitudinal scale size). Following geometrical arguments, the distance that electrons drift east in a single bounce is a product of the circumference of the drift shell foot print, and the fraction of the total drift orbit traversed in a single bounce and is given by,

$$d_{az} = 2\pi(R_E + A) \cos(\lambda) \frac{t_b}{\langle T_d \rangle} \quad (1)$$

where  $R_E$  is the Earth's radius,  $A$  is the spacecraft altitude,  $\lambda$  is the magnetic latitude,  $t_b$  is the electron bounce period, and  $\langle T_d \rangle$  is the electron drift period. Parks [2003] derived  $\langle T_d \rangle$  to be,

$$\langle T_d \rangle \approx \begin{cases} 43.8/(L \cdot E) & \text{if } \alpha_0 = 90^\circ \\ 62.7/(L \cdot E) & \text{if } \alpha_0 = 0^\circ \end{cases} \quad (2)$$

where  $E$  is the electron energy in MeV,  $L$  is the L shell, and  $\alpha_0$  is the equatorial pitch angle. Electrons mirroring at FIREBIRD-II have  $\alpha_0 \approx 3.7^\circ$  and so the  $\alpha_0 = 0^\circ$  limit was used.

The microburst's longitudinal scale size is defined as the distance the highest energy electrons drifted in the time between the observations of the first and last peaks. This scale size is given by  $D_{az} = n d_{az}$  where  $n$  is the number of bounces observed. The stars in Fig. 3 (with labels corresponding to energy channel boundaries) represent the locations when the microburst was observed at P1, such that an electron of that energy would drift eastward to be seen at P5 for FU3 and P4 for FU4. (Added: Since FU3 observed more peaks it observed) the larger longitudinal scale size (Replaced: ~~was observed by FU3 and~~ replaced with: which) is shown with the red dashed box in Fig. 3. (Replaced: ~~The minimum scale size was  $39 \pm 1$  km for the 555 keV electrons and  $51 \pm 1$  km for the 771 keV electrons (lower and upper bound of the fourth energy channel)~~ replaced with: FU3's fourth energy channel's bounds are 555 keV and 771 keV, which correspond to longitudinal distances of  $39 \pm 1$  km and  $51 \pm 1$ , respectively). The uncertainty was estimated by propagating the uncertainty in



the bounce time Eq. 1. (Added: While the observed minimum longitudinal scale size is dependent on FIREBIRD-II's energy channels, the true scale size may not be.)

To investigate how the microburst scale size (Replaced: ~~relates to the generation mechanism near the magnetic equator~~ replaced with: ~~compares to the scale sizes of chorus waves near the magnetic equator~~), the microburst's longitudinal and latitudinal scale sizes and their uncertainties in LEO were mapped to the magnetic equator with T89. The radial scale size (latitudinal scale mapped from LEO) was greater than  $500 \pm 10$  km. The azimuthal scale size (longitudinal scale mapped from LEO) of 555 keV electrons was greater than  $450 \pm 10$  km and for the 771 keV electrons it was greater than  $530 \pm 10$  km. (Added: The lower bound microburst scale size is similar to the chorus scale sizes derived by *Agapitov et al.* [2011, 2017], and is discussed below.)

#### 4 Discussion and Conclusions

We presented the first observation of a large microburst with multiple bounces made possible by the twin FIREBIRD-II CubeSats. The microburst's lower bound LEO latitudinal and longitudinal scale sizes of  $29 \pm 1$  km and  $51 \pm 1$  km make it one of the largest observed. The microburst's LEO scale size was larger than the latitudinal scale sizes of typical  $> 1$  MeV microbursts reported in *Blake et al.* [1996], approximately 10 times larger than reported in *Dietrich et al.* [2010], and approximately 2.6 times larger than other simultaneous microbursts observed by FIREBIRD-II [*Crew et al.*, 2016]. Lastly, the scale sizes derived here were similar to the scale sizes of  $> 15$  keV microbursts observed with a high altitude balloon [*Parks*, 1967]. No energy dependence on the (Added: minimum latitudinal) scale size was observed, (Added: while the observed energy dependence of the minimum longitudinal scale size is an artifact of the technique we used to estimate their drift motion).

The microburst scale size obtained in Section 3.3 and scaled to the geomagnetic equator can be compared with the scales of chorus waves presumably responsible for the rapid burst electron precipitation. Early direct estimates of the chorus source scales were made by the coordinated measurement by ISEE-1, 2. The wave power correlation scale was estimated to be about several hundred kilometers across the background magnetic field [*Gurnett et al.*, 1979]. Furthermore, *Santolik et al.* [2003] determined the correlation lengths of chorus-type whistler waves to be around 100 km based on multipoint CLUSTER Wide Band Data measurements near the chorus source region at  $L \approx 4$ , during the magnetic storm of 18 April

2002. Agapitov *et al.* [2010, 2011, 2017] recently showed that the spatial extent of chorus  
 source region can be larger, ranging from 600 km in the outer radiation belt to more than  
 1000 km in the outer magnetosphere. The lower bound azimuthal and latitudinal scales ob-  
 tained in Section 3.3 and scaled to the magnetic equator, are similar to the whistler-mode  
 chorus source scale sizes reported in Agapitov *et al.* [2011, 2017].

No wave measurements from nearby spacecraft were available at this time. Neverthe-  
 less, during the hours before and after this observation, the Van Allen Probes' [Mauk *et al.*,  
 2013] Electric and Magnetic Field Instrument and Integrated Science [Kletzing *et al.*, 2013]  
 observed strong wave power in the lower band chorus frequency range, inside the outer ra-  
 diation belt between 22 and 2 MLT. Furthermore, AE  $\sim$  400 nT at this time, and relatively  
 strong chorus waves were statistically more likely to be present at FIREBIRD-II's MLT [Li  
*et al.*, 2009].

The empirically estimated and modeled  $t_b$  in this study agree within FIREBIRD-II's  
 uncertainties, confirming that the energy-dependent dispersion was due to bouncing. The  
 $t_b$  curves are a proxy for field line length, and this agreement implies that they are compa-  
 rable. This is expected since the magnetosphere is not drastically compressed at 8 MLT, but  
 we expect a larger discrepancy near midnight, where the magnetosphere is more stretched  
 and difficult to accurately model. (Replaced: This analysis can be used as a diagnostic tool to  
 validate field line lengths in future studies; replaced with: In future studies, this analysis can  
 be used as a diagnostic tool to validate field line lengths, and improve magnetic field mod-  
 els.)

The similarity of the microburst and chorus source region scale sizes, as well as mag-  
 netospheric location and conditions, further support the causal relationship between mi-  
 crobursts and chorus.

## Acknowledgments

This work was made possible with help from the FIREBIRD team, and the members of the  
 Space Sciences and Engineering Laboratory at Montana State University for their hard work  
 to make this mission a success. In addition, M. Shumko acknowledges Drew Turner for his  
 suggestions regarding the bounce period calculations, and Dana Longcope for his proofread-  
 ing feedback. The FIREBIRD-II data are available at [http://solar.physics.montana.edu/FIREBIRD\\_II/](http://solar.physics.montana.edu/FIREBIRD_II/).  
 This analysis is supported by the National Science Foundation under Grant Numbers 0838034

and 1339414. Furthermore, the work of O. Agapitov was supported by the NASA grant NNX16AF85G.

## References

- Abel, B., and R. M. Thorne (1998), Electron scattering loss in earth's inner magnetosphere: 1. dominant physical processes, *Journal of Geophysical Research: Space Physics*, *103*(A2), 2385–2396.
- Agapitov, O., V. Krasnoselskikh, Y. Zaliznyak, V. Angelopoulos, O. Le Contel, and G. Rolland (2010), Chorus source region localization in the earth's outer magnetosphere using themis measurements, *Annales Geophysicae*, *28*(6), 1377–1386, doi:10.5194/angeo-28-1377-2010.
- Agapitov, O., V. Krasnoselskikh, T. Dudok de Wit, Y. Khotyaintsev, J. S. Pickett, O. Santolik, and G. Rolland (2011), Multispacecraft observations of chorus emissions as a tool for the plasma density fluctuations' remote sensing, *Journal of Geophysical Research: Space Physics*, *116*(A9), n/a–n/a, doi:10.1029/2011JA016540, a09222.
- Agapitov, O., L. W. Blum, F. S. Mozer, J. W. Bonnell, and J. Wygant (2017), Chorus whistler wave source scales as determined from multipoint van allen probe measurements, *Geophysical Research Letters*, pp. n/a–n/a, doi:10.1002/2017GL072701, 2017GL072701.
- Anderson, B., S. Shekhar, R. Millan, A. Crew, H. Spence, D. Klumpar, J. Blake, T. O'Brien, and D. Turner (2017), Spatial scale and duration of one microburst region on 13 august 2015, *Journal of Geophysical Research: Space Physics*.
- Anderson, K. A., and D. W. Milton (1964), Balloon observations of x rays in the auroral zone: 3. high time resolution studies, *Journal of Geophysical Research*, *69*(21), 4457–4479, doi:10.1029/JZ069i021p04457.
- Blake, J., M. Looper, D. Baker, R. Nakamura, B. Klecker, and D. Hovestadt (1996), New high temporal and spatial resolution measurements by sampex of the precipitation of relativistic electrons, *Advances in Space Research*, *18*(8), 171 – 186, doi: [http://dx.doi.org/10.1016/0273-1177\(95\)00969-8](http://dx.doi.org/10.1016/0273-1177(95)00969-8).
- Blum, L., X. Li, and M. Denton (2015), Rapid mev electron precipitation as observed by sampex/hilt during high-speed stream-driven storms, *Journal of Geophysical Research: Space Physics*, *120*(5), 3783–3794, doi:10.1002/2014JA020633, 2014JA020633.
- Boscher, D., S. Bourdarie, P. O'Brien, T. Guild, and M. Shumko (2012), Irbem-lib library.

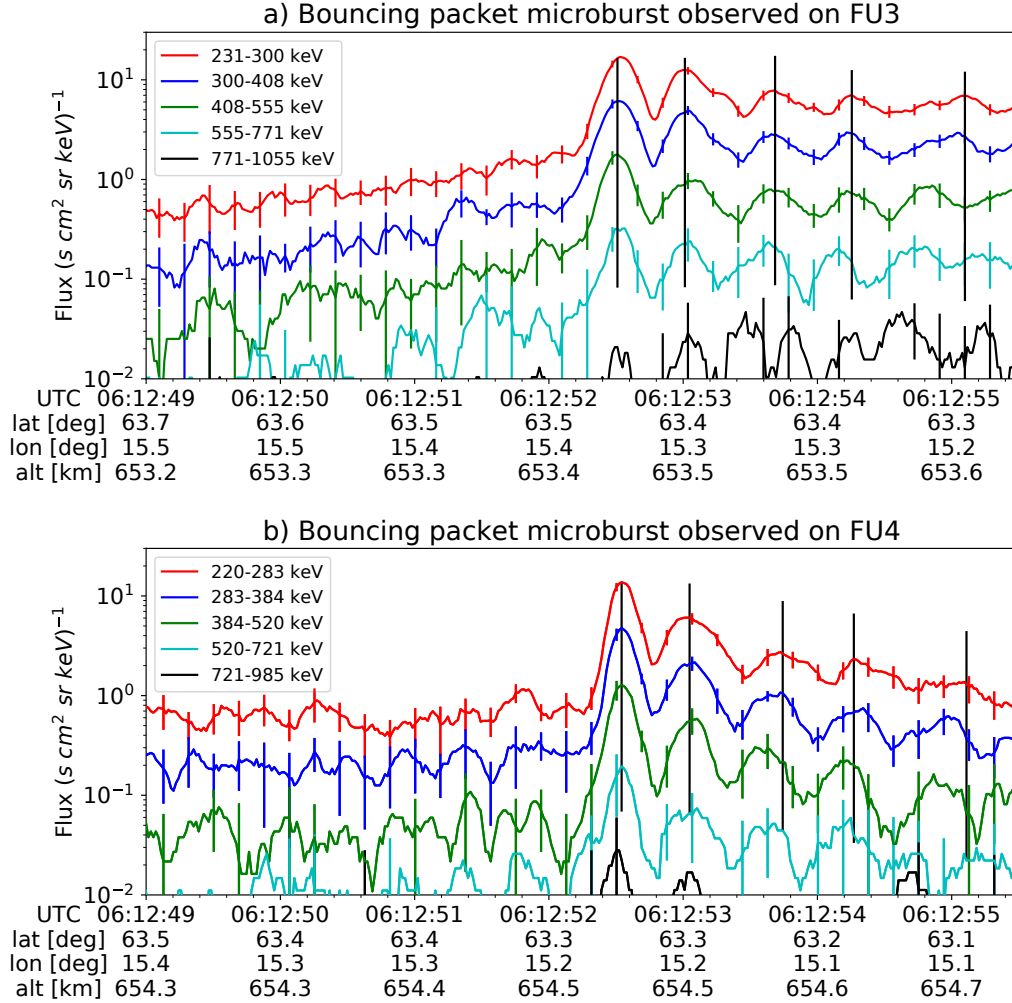


**Figure 1.** HiRes data of the microburst observed at February 2nd, 2015 at 06:12:53 UT, smoothed with a 150 ms rolling average. The subsequent bounces showed some energy dispersion. As discussed in the supporting information, a time correction of -2.28 s was applied to FU3. While the flux from five energy channels is shown, only channels with reasonable counting statistics were used for the spatial scale analysis. Vertical colored bars show the  $\sqrt{N}$  error every 10th data point and vertical black bars are lined up with the peaks in the 220-283 keV energy channel to help identify dispersion.

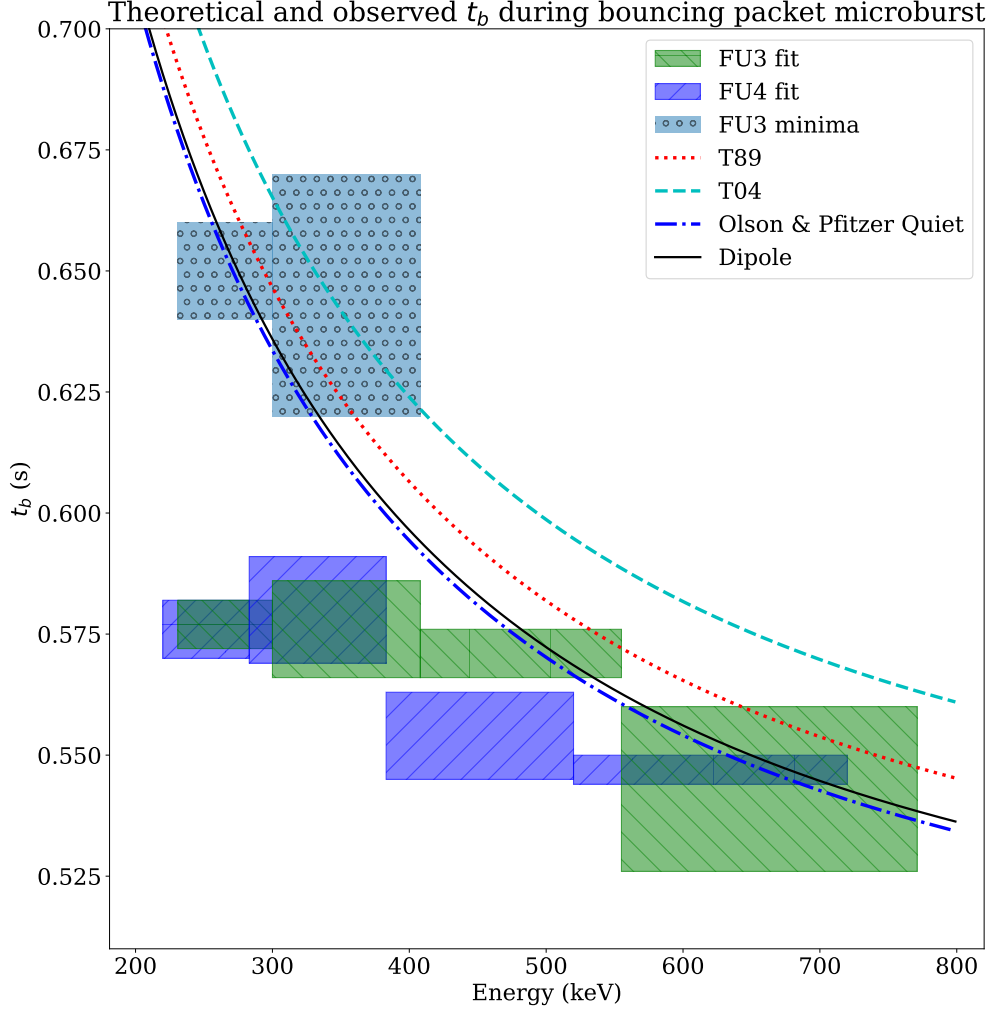


**Figure 2.** Observed and theoretical  $t_b$  for electrons of energies from 200 to 770 keV. The solid black line is  $t_b$  in a dipole magnetic field, derived in *Schulz and Lanzerotti* [1974]. The red dotted and cyan dashed lines are the  $t_b$  derived using the T89, and T04 magnetic field models with IRBEM-Lib. Lastly, the blue dot-dash curve is the  $t_b$  derived using the Olson & Pfitzer Quiet model. The green and purple rectangles represent the observed  $t_b$  for FU3 and FU4 using a Gaussian fit, respectively. The blue rectangles represent the observed  $t_b$  calculated with the minima between the bounces. The width of the boxes represent the width of those energy channels, and the height represents the uncertainty from the fit.

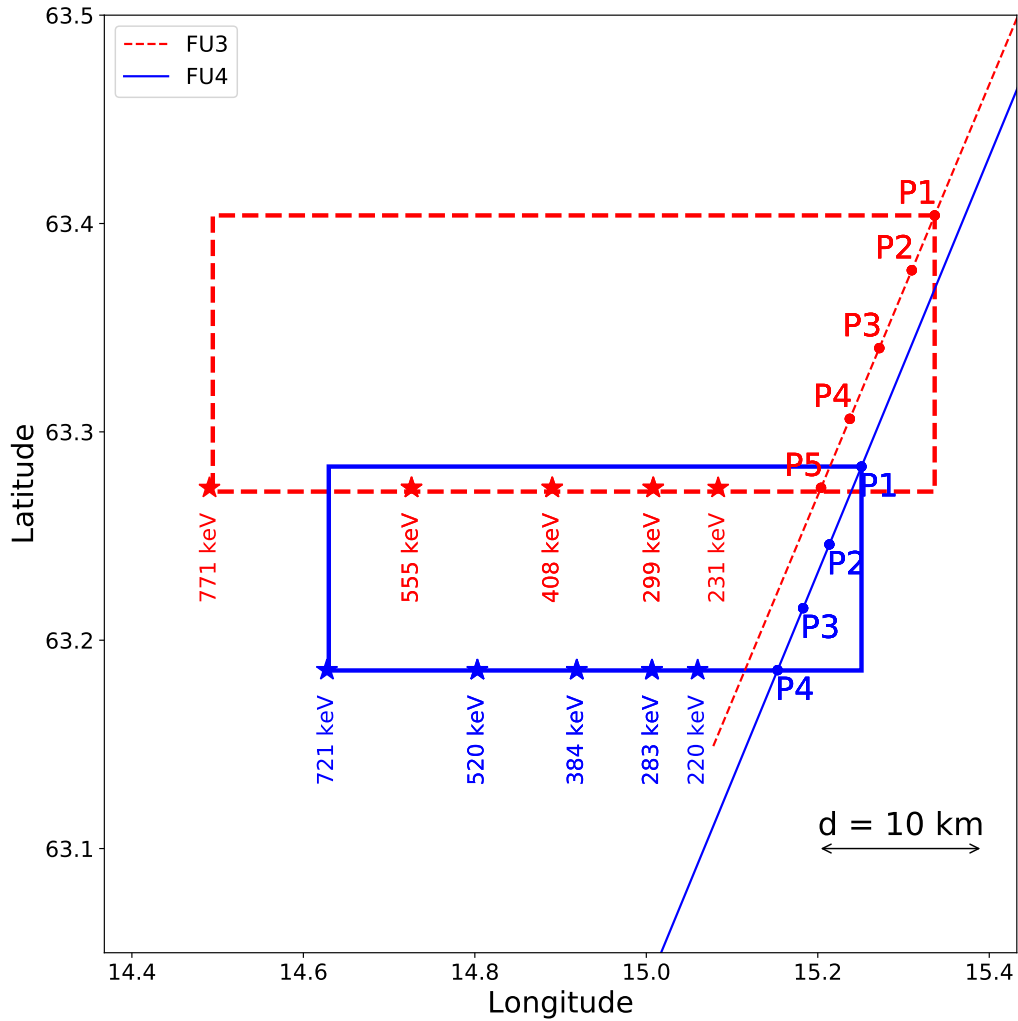


**Figure 3.** The topology of the FIREBIRD-II orbit and the multiple bounces of the microburst projected onto latitude and longitude with axis scaled to equal distance. Attributes relating to FU3 shown in red dashed lines, and FU4 with blue solid lines. The spacecraft path is shown with the diagonal lines, starting at the upper right corner. The labels P1-4 for FU4 and P1-5 for FU3 indicate where the spacecraft were when the  $N^{th}$  peak was seen in the lowest energy channel in the HiRes data. The stars with the accompanying energy labels represent the locations of the electrons with that energy that started at time of P1, and were seen at the last peak on each spacecraft. The rectangles represent the lower bound of the microburst scale size, assuming that the majority of the electrons were in the upper boundary of energy channel 4.

- 348 Breneman, A., A. Crew, J. Sample, D. Klumpar, A. Johnson, O. Agapitov, M. Shumko,  
349 D. Turner, O. Santolik, J. Wygant, et al. (2017), Observations directly linking relativistic  
350 electron microbursts to whistler mode chorus: Van allen probes and firebird ii, *Geophysi-  
351 cal Research Letters*.
- 352 Comess, M., D. Smith, R. Selesnick, R. Millan, and J. Sample (2013), Duskside relativistic  
353 electron precipitation as measured by sampex: A statistical survey, *Journal of Geophysical  
354 Research: Space Physics*, 118(8), 5050–5058, doi:10.1002/jgra.50481.
- 355 Crew, A. B., H. E. Spence, J. B. Blake, D. M. Klumpar, B. A. Larsen, T. P. O’Brien,  
356 S. Driscoll, M. Handley, J. Legere, S. Longworth, K. Mashburn, E. Mosleh, N. Ryha-  
357 jlo, S. Smith, L. Springer, and M. Widholm (2016), First multipoint in situ observations  
358 of electron microbursts: Initial results from the nsf firebird ii mission, *Journal of Geo-  
359 physical Research: Space Physics*, 121(6), 5272–5283, doi:10.1002/2016JA022485,  
360 2016JA022485.
- 361 Datta, S., R. Skoug, M. McCarthy, and G. Parks (1997), Modeling of microburst electron  
362 precipitation using pitch angle diffusion theory, *Journal of Geophysical Research: Space  
363 Physics*, 102(A8), 17,325–17,333.
- 364 Dietrich, S., C. J. Rodger, M. A. Clilverd, J. Bortnik, and T. Raita (2010), Relativistic mi-  
365 croburst storm characteristics: Combined satellite and ground-based observations, *Journal  
366 of Geophysical Research: Space Physics*, 115(A12).
- 367 Fang, X., C. E. Randall, D. Lummerzheim, W. Wang, G. Lu, S. C. Solomon, and R. A.  
368 Frahm (2010), Parameterization of monoenergetic electron impact ionization, *Geophysi-  
369 cal Research Letters*, 37(22).
- 370 Gurnett, D., R. Anderson, F. Scarf, R. Fredricks, and E. Smith (1979), Initial results from the  
371 isee-1 and-2 plasma wave investigation, *Space Science Reviews*, 23(1), 103–122.
- 372 Horne, R. B., and R. M. Thorne (2003), Relativistic electron acceleration and precipitation  
373 during resonant interactions with whistler-mode chorus, *Geophysical Research Letters*,  
374 30(10), n/a–n/a, doi:10.1029/2003GL016973, 1527.
- 375 Kletzing, C., W. Kurth, M. Acuna, R. MacDowall, R. Torbert, T. Averkamp, D. Bodet,  
376 S. Bounds, M. Chutter, J. Connerney, et al. (2013), The electric and magnetic field in-  
377 strument suite and integrated science (emfisis) on rbsp, *Space Science Reviews*, 179(1-4),  
378 127–181.
- 379 Klumpar, D., L. Springer, E. Mosleh, K. Mashburn, S. Berardinelli, A. Gunderson,  
380 M. Handly, N. Ryhajlo, H. Spence, S. Smith, J. Legere, M. Widholm, S. Longworth,

- 381 A. Crew, B. Larsen, J. Blake, and N. Walmsley (2015), Flight system technologies en-  
382 abling the twin-cubesat firebird-ii scientific mission.
- 383 Lee, J.-J., G. K. Parks, K. W. Min, H. J. Kim, J. Park, J. Hwang, M. P. McCarthy, E. Lee,  
384 K. S. Ryu, J. T. Lim, E. S. Sim, H. W. Lee, K. I. Kang, and H. Y. Park (2005), Energy  
385 spectra of 170-360 keV electron microbursts measured by the Korean STSAT-1, *Geophysical*  
386 *Research Letters*, 32(13), doi:10.1029/2005GL022996, 113106.
- 387 Lee, J. J., G. K. Parks, E. Lee, B. T. Tsurutani, J. Hwang, K. S. Cho, K.-H. Kim, Y. D. Park,  
388 K. W. Min, and M. P. McCarthy (2012), Anisotropic pitch angle distribution of 100 keV  
389 microburst electrons in the loss cone: measurements from STSAT-1, *Annales Geophysicae*,  
390 30(11), 1567–1573, doi:10.5194/angeo-30-1567-2012.
- 391 Li, W., R. M. Thorne, V. Angelopoulos, J. Bortnik, C. M. Cully, B. Ni, O. LeContel,  
392 A. Roux, U. Auster, and W. Magnes (2009), Global distribution of whistler-mode chorus  
393 waves observed on the THEMIS spacecraft, *Geophysical Research Letters*, 36(9), n/a–n/a,  
394 doi:10.1029/2009GL037595, 109104.
- 395 Lorentzen, K. R., J. B. Blake, U. S. Inan, and J. Bortnik (2001a), Observations of relativis-  
396 tic electron microbursts in association with VLF chorus, *Journal of Geophysical Research:*  
397 *Space Physics*, 106(A4), 6017–6027, doi:10.1029/2000JA003018.
- 398 Lorentzen, K. R., M. D. Looper, and J. B. Blake (2001b), Relativistic electron mi-  
399 crobursts during the geomagnetic storms, *Geophysical Research Letters*, 28(13), 2573–2576, doi:  
400 10.1029/2001GL012926.
- 401 Mauk, B., N. J. Fox, S. Kanekal, R. Kessel, D. Sibeck, and A. Ukhorskiy (2013), Science ob-  
402 jectives and rationale for the radiation belt storm probes mission, *Space Science Reviews*,  
403 179(1-4), 3–27.
- 404 Meredith, N., R. Horne, D. Summers, R. Thorne, R. Iles, D. Heynderickx, and R. Ander-  
405 son (2002), Evidence for acceleration of outer zone electrons to relativistic energies by  
406 whistler mode chorus, in *Annales Geophysicae*, vol. 20, pp. 967–979.
- 407 Millan, R., and R. Thorne (2007), Review of radiation belt relativistic electron losses,  
408 *Journal of Atmospheric and Solar-Terrestrial Physics*, 69(3), 362 – 377, doi:  
409 <http://dx.doi.org/10.1016/j.jastp.2006.06.019>, Global Aspects of Magnetosphere-  
410 Ionosphere Coupling Global Aspects of Magnetosphere-Ionosphere Coupling.
- 411 Millan, R. M., R. Lin, D. Smith, K. Lorentzen, and M. McCarthy (2002), X-ray observations  
412 of MeV electron precipitation with a balloon-borne germanium spectrometer, *Geophysical*  
413 *Research Letters*, 29(24).



- 414 Mozer, F. S., O. V. Agapitov, J. B. Blake, and I. Y. Vasko (2018), Simultaneous observations  
415 of lower band chorus emissions at the equator and microburst precipitating electrons in  
416 the ionosphere, *Geophysical Research Letters*, pp. n/a–n/a, doi:10.1002/2017GL076120,  
417 2017GL076120.
- 418 Nakamura, R., D. N. Baker, J. B. Blake, S. Kanekal, B. Klecker, and D. Hovestadt (1995),  
419 Relativistic electron precipitation enhancements near the outer edge of the radiation belt,  
420 *Geophysical Research Letters*, 22(9), 1129–1132, doi:10.1029/95GL00378.
- 421 Nakamura, R., M. Isowa, Y. Kamide, D. Baker, J. Blake, and M. Looper (2000), Observa-  
422 tions of relativistic electron microbursts in association with vlf chorus, *J. Geophys. Res.*,  
423 105, 15,875–15,885.
- 424 O’Brien, T. P., K. R. Lorentzen, I. R. Mann, N. P. Meredith, J. B. Blake, J. F. Fennell, M. D.  
425 Looper, D. K. Milling, and R. R. Anderson (2003), Energization of relativistic elec-  
426 trons in the presence of ulf power and mev microbursts: Evidence for dual ulf and vlf  
427 acceleration, *Journal of Geophysical Research: Space Physics*, 108(A8), n/a–n/a, doi:  
428 10.1029/2002JA009784, 1329.
- 429 O’Brien, T. P., M. D. Looper, and J. B. Blake (2004), Quantification of relativistic electron  
430 microburst losses during the gem storms, *Geophysical Research Letters*, 31(4), n/a–n/a,  
431 doi:10.1029/2003GL018621, 104802.
- 432 Olson, W. P., and K. A. Pfizter (1982), A dynamic model of the magnetospheric magnetic  
433 and electric fields for july 29, 1977, *Journal of Geophysical Research: Space Physics*,  
434 87(A8), 5943–5948, doi:10.1029/JA087iA08p05943.
- 435 Parks, G. (2003), *Physics Of Space Plasmas: An Introduction, Second Edition*, Westview  
436 Press.
- 437 Parks, G. K. (1967), Spatial characteristics of auroral-zone x-ray microbursts, *Journal of*  
438 *Geophysical Research*, 72(1), 215–226.
- 439 Santolik, O., D. Gurnett, J. Pickett, M. Parrot, and N. Cornilleau-Wehrin (2003), Spatio-  
440 temporal structure of storm-time chorus, *Journal of Geophysical Research: Space*  
441 *Physics*, 108(A7).
- 442 Schulz, M., and L. J. Lanzerotti (1974), *Particle Diffusion in the Radiation Belts*, Springer.
- 443 Selesnick, R. S., J. B. Blake, and R. A. Mewaldt (2003), Atmospheric losses of radia-  
444 tion belt electrons, *Journal of Geophysical Research: Space Physics*, 108(A12), doi:  
445 10.1029/2003JA010160, 1468.

- 446 Shprits, Y. Y., and R. M. Thorne (2004), Time dependent radial diffusion modeling of rel-  
447 ativistic electrons with realistic loss rates, *Geophysical Research Letters*, *31*(8), n/a–n/a,  
448 doi:10.1029/2004GL019591, 108805.
- 449 Shprits, Y. Y., N. P. Meredith, and R. M. Thorne (2007), Parameterization of radiation belt  
450 electron loss timescales due to interactions with chorus waves, *Geophysical Research Let-*  
451 *ters*, *34*(11), n/a–n/a, doi:10.1029/2006GL029050, 111110.
- 452 Spence, H. E., J. B. Blake, A. B. Crew, S. Driscoll, D. M. Klumpar, B. A. Larsen, J. Legere,  
453 S. Longworth, E. Mosleh, T. P. O’Brien, S. Smith, L. Springer, and M. Widholm (2012),  
454 Focusing on size and energy dependence of electron microbursts from the van allen radia-  
455 tion belts, *Space Weather*, *10*(11), doi:10.1029/2012SW000869.
- 456 Summers, D., R. M. Thorne, and F. Xiao (1998), Relativistic theory of wave-particle reso-  
457 nant diffusion with application to electron acceleration in the magnetosphere, *Journal of*  
458 *Geophysical Research: Space Physics*, *103*(A9), 20,487–20,500.
- 459 Thorne, R. M. (2010), Radiation belt dynamics: The importance of wave-particle interac-  
460 tions, *Geophysical Research Letters*, *37*(22), doi:10.1029/2010GL044990, 122107.
- 461 Thorne, R. M., T. P. O’Brien, Y. Y. Shprits, D. Summers, and R. B. Horne (2005), Timescale  
462 for mev electron microburst loss during geomagnetic storms, *Journal of Geophysical Re-*  
463 *search: Space Physics*, *110*(A9), n/a–n/a, doi:10.1029/2004JA010882, a09202.
- 464 Tsyganenko, N. (1989), A solution of the chapman-ferraro problem for an ellip-  
465 soidal magnetopause, *Planetary and Space Science*, *37*(9), 1037 – 1046, doi:  
466 [http://dx.doi.org/10.1016/0032-0633\(89\)90076-7](http://dx.doi.org/10.1016/0032-0633(89)90076-7).
- 467 Tsyganenko, N. A., and M. I. Sitnov (2005), Modeling the dynamics of the inner magne-  
468 tosphere during strong geomagnetic storms, *Journal of Geophysical Research: Space*  
469 *Physics*, *110*(A3), n/a–n/a, doi:10.1029/2004JA010798, a03208.
- 470 Ukhorskiy, A. Y., B. J. Anderson, P. C. Brandt, and N. A. Tsyganenko (2006), Storm time  
471 evolution of the outer radiation belt: Transport and losses, *Journal of Geophysical Re-*  
472 *search: Space Physics*, *111*(A11), n/a–n/a, doi:10.1029/2006JA011690, a11S03.
- 473 Woodger, L., A. Halford, R. Millan, M. McCarthy, D. Smith, G. Bowers, J. Sample, B. An-  
474 derson, and X. Liang (2015), A summary of the barrel campaigns: Technique for studying  
475 electron precipitation, *Journal of Geophysical Research: Space Physics*, *120*(6), 4922–  
476 4935.